Marine Environmental Research 170 (2021) 105447

Contents lists available at ScienceDirect

Marine Environmental Research

journal homepage: www.elsevier.com/locate/marenvrev

Ocean acidification exacerbates copper toxicity in both juvenile and adult stages of the green tide alga *Ulva linza*

Tianpeng Xu [a], Junyang Cao [a], Rui Qian [a], Yujing Song [a], Wen Wang [a], Jing Ma [a,*], Kunshan Gao [d], Juntian Xu [a,b,c]

[a] Jiangsu Key Lab of Marine Bioresources and Environment/Jiangsu Key Lab of Marine Biotechnology, Jiangsu Ocean University, Lianyungang, 222005, China
[b] Co-Innovation Center of Jiangsu Marine Bio-industry Technology, Lianyungang, 222005, China
[c] State Key Lab of Marine Environmental Science, Xiamen University, Xiamen, 361102, China
[d] State Key Laboratory of Marine Environmental Science, Xiamen University/College of Ocean and Earth Sciences, Xiamen, 361005, China

ARTICLE INFO

Keywords:
Photosynthetic performance
Seawater acidification
Copper
Life period
Ulva linza

ABSTRACT

The toxicity of heavy metals to coastal organisms can be modulated by changes in pH due to progressive ocean acidification (OA). We investigated the combined impacts of copper and OA on different stages of the green macroalga *Ulva linza*, which is widely distributed in coastal waters, by growing the alga under the addition of Cu (control, 0.125 (medium, MCu), and 0.25 (high) μM, HCu) and elevated pCO_2 of 1,000 μatm, predicted in the context of global change. The relative growth rates decreased significantly in both juvenile and adult thalli at HCu under OA conditions. The net photosynthetic and respiration rates, as well as the relative electron transfer rates for the adult thalli, also decreased under the combined impacts of HCu and OA, although no significant changes in the contents of photosynthetic pigments were detected. Our results suggest that Cu and OA act synergistically to reduce the growth and photosynthetic performance of *U. linza*, potentially prolonging its life cycle.

1. Introduction

As a result of the combustion of fossil fuels and deforestation, the CO_2 concentration in the atmosphere rapidly increased from 280 in the preindustrial era to about 415 μatm today (https://www.co2.earth/). It is predicted to reach 1,000 μatm by the end of this century (https://www.ipcc.ch/reports/). The increased CO_2 deposition into seawater will result in a pH decrease of 0.14–0.41 units by 2100 and 0.3–0.7 units by 2300 (Doney et al., 2009), the so-called "ocean acidification" (OA). The input of large amounts of CO_2 and their dissolution in seawater also lead to changes in the carbonate chemistry (Doney et al., 2009).

While OA can affect many organisms (Ji and Gao, 2020), its effects on macroalgae can be positive, neutral, and negative in different stages of their life cycles and/or in combination with other factors (Xu and Gao, 2012; Gao et al., 2016a, b; Qu et al., 2017; Bao et al., 2019; Yue et al., 2019; Ji and Gao, 2020). Generally, fleshy macroalgae experience diel pH changes in coastal waters and can tolerate pH decreases associated with OA, and the increased CO_2 availability can facilitate their growth (Gao et al., 1991; Xu and Gao, 2012). Such enhancement can be moderated by other factors, such as light levels and/or daytime length, temperature, and solar UV (Gao et al., 2010; Yue et al., 2019; Ji and Gao, 2020; Wang et al., 2020). In waters surrounding CO_2 seeps, green macroalgae grow well in the acidified seawater (Hall-Spencer et al., 2008; Hall-Spencer and Harvey, 2019). However, relatively little is known about the combined impacts of OA and heavy metals, whose ionic properties might be altered by pH changes (MillerO et al., 2009; Richards et al., 2011; Hoffmann et al., 2012; Zeng et al., 2015). Plants of the genus *Ulva* increase their growth rates with enhanced electron transport and non-photochemical quenching, and the down-regulated CO_2-concentrating mechanisms and enhanced photorespiration play important roles against acidic stress (Xu and Gao, 2012). However, with the addition of other stressors, their physiological performance can be altered. Gao et al. (2016a) showed that OA and light stress suppressed net photosynthetic rates of *Ulva* plants, and OA inhibited the growth of *U. linza* under nutrient limitation, which, however, rarely occurs in coastal waters (Gao et al., 2018).

During the past half-century, along with the rapid economic development, pollution with heavy metals such as mercury (Hg), copper (Cu),

* Corresponding author.
E-mail address: jingma@jou.edu.cn (J. Ma).

https://doi.org/10.1016/j.marenvres.2021.105447
Received 18 May 2021; Received in revised form 20 July 2021; Accepted 5 August 2021
Available online 12 August 2021

lead (Pb), nickel (Ni), cadmium (Cd), zinc (Zn), and iron (Fe) have become a global concern (Andrade et al., 2004; Iheanacho et al., 2017; Mirzaei et al., 2016). As they are persistent in the environment and toxic (Leusch et al., 1995), they cause severe damage to aquatic organisms and affect human beings health through the food chain (Ndu et al., 2016). Macroalgae are mainly distributed in coastal waters and can be sensitive to heavy metal pollution (Naser, 2013; Ismail and Ismail, 2017). Among the above-mentioned heavy metals, Cu is a common contaminant in marine environments and has become a local stressor (Boyer and Brand, 1998). According to previous studies, the Cu concentration is 0.02 μM in the natural seawater (Gao et al., 2017), with a maximum of 1.01 μM (Figueira et al., 2016). In another study, *Ulva intestinalis* accumulated high levels of Cu, followed by Pb, Zn, Cr, and Cd (Baumann et al., 2009). In the green tide alga *Ulva prolifera*, the Cu ion concentration in seawater of 0.50 mg L^{-1} significantly decreased photosynthesis and growth, causing morphological abnormalities (Gao et al., 2017).

In recent years, the impacts of OA on marine organisms and ecosystems had been a topic of global concern, especially in the context of multiple driver effects (Gao et al., 2012, 2019; Schlüter et al., 2016; Kang et al., 2021). Sensitivities to OA may differ among species and even among life stages of the same species (Isari et al., 2015). *Ulva linza*, one of the most common green algae, played an important role in the food, chemical, and pharmaceutical industries (Koch et al., 2013) and was used a raw material for bioremediation and biofuel feedstock (Shi et al., 2017; Golubkov et al., 2018). It reproduces throughout the year, with faster germination from its spores during May–July in the northern part of China. While juvenile stage of some brown macroalgae was more sensitive to OA when also subjected to other stressors (Ji and Gao, 2020), OA and warming inhibited the early development of the giant kelp *Macrocystis pyrifera*, lowering germination rates and increasing spore mortality (Gaitán-Espitia et al., 2014). The 2013 IPCC report indicated that the average global and ocean temperature has increased by 0.85 °C from 1880 to 2012 (Stocker et al., 2014). On a global scale, the most significant ocean warming occurred in the ocean surface water (above 75 m). From 1971 to 2010, the ocean surface (above 75 m) temperature has increased by 0.11 °C, and it is expected that by the end of this century, the sea surface temperature will increase by 1.2–3.2 °C.

Against this background, we took Cu as an additional stressor to investigate the combined effects of OA and heavy metals. Since the toxicity of Cu differs at different pH levels, pH decrease along with elevated CO_2 concentrations can affect algal responses (Gao et al., 2017). Therefore, we hypothesized that the combination of OA and Cu can reduce *Ulva linza* growth, in particular when in the juvenile stage. We tested this hypothesis by growing *U. linza* under different levels of Cu and CO_2, measuring its growth rate, photosynthetic rate, and pigment content after 17 days.

2. Materials and methods

2.1. Sample collection and culture conditions

Ulva linza was collected from the intertidal zone of Liandao Island (119.3 °E, 34.5 °N), Lianyungang, Jiangsu Province, China, in January 2017. The sampled healthy thalli were cleaned with filtered sterile seawater and then precultured in an intelligent illumination incubator (Jiangnan GXZ-300C, Ningbo, China). Filtered sterile seawater, with 60 μM $NaNO_3$ and 8.0 μM NaH_2PO_4, was used to culture the thalli. The photosynthetically active radiation in the incubator was 150 μmol photons m^{-2} s^{-1} (12 h:12 h), at a temperature of 20 °C. The natural seawater was sourced from the sampling point, and the supplemented nutrient content was similar to the seawater in terms of nitrogen and phosphorus levels. The seawater in the glass bottles was renewed every two days. After the thalli had released spores, these were inoculated onto glass slides and cultured under preculture conditions. Subsequently, the thalli were treated with different Cu concentrations (control, LCu; 0.125, MCu; and 0.25 μM, HCu) and two CO_2 concentrations (atmospheric CO_2 concentration, 415 μatm, LC; high CO_2 concentration, 1,000 μatm, HC) for long-term experiments over 17 d. The Cu concentration was 0.02 μM in the natural seawater, which was used as control without adding $CuSO_4$. The Cu concentrations were selected according to Gao et al. (2017) and measured by inductively-coupled plasma atomic emission spectrometry (ICP-AES) (AA240FS, Varian, California, USA). The method of testing Cu complied with the regulations to reduce the risk of metal contamination (Leal et al., 2016). The 415-μatm CO_2 was prepared by pumping atmospheric air, and 1, 000-μatm CO_2 was achieved by a CO_2 plant chamber (HP1000G-D, Wuhan Ruihua Instruction and Equipment Ltd., Wuhan, China). In the LC and HC cultures, we maintained pH levels of 8.18 and 7.83, respectively; variations remained below 0.05. Thalli lengths shorter than 1 cm defined the juvenile stage, and thalli lengths exceeding 1 cm indicated the adult stage. Over time, the branches of the thalli increased, and the length could not be measured anymore; this stage was regarded as the late adult stage. The biomass density of thalli was adjusted for each treatment to maintain the stability of the carbonate system. Each treatment contained three replications.

2.2. Measurement of growth

At the juvenile stage, the length was measured via a microscope (DM 500, Leica, Germany) with a stereo camera. When the length of the algae was beyond 1 cm, the thalli were removed from the glass slides, and their lengths every 2 days using a ruler. At about 10 days, when the algae had grown to 1 cm, the calculated relative growth rate (RGR) was determined for the juvenile stage. When the length exceeded 1 cm at about 15 or 17 days, and the RGR showed a stable trend, the adult stage was reached. At the late adult growth stage, the relative growth rate (RGR) was also calculated by measuring the fresh weight of the algae, using the following equation:

$$RGR = 100 \times (\ln L_t - \ln L_o) / t, \text{ or } RGR = 100 \times (\ln M_t - \ln M_o) / t, \quad (1)$$

where L_o or M_o represents the initial length or fresh weight of the algae, respectively, and L_t or M_t represents the length or fresh weight of algae after t days, respectively.

2.3. Photosynthesis and respiration measurements

The net photosynthetic rate and the respiration rate of the algae were measured between 9:00 a.m. and 3:00 p.m. by a Clark-type oxygen electrode (YSI Model 5300A, YSI Incorporated, Yellow Springs, Ohio, USA). The thalli were cut into about 1-cm-long pieces and subjecting to the cultivation conditions described above for about 1 h to avoid cutting damage. Subsequently, thalli with a fresh weight of approximately 0.02 g were transferred to a photosynthetic chamber containing 8 mL cultured seawater. The temperature and irradiance conditions were as described above. The measurement was conducted within 5 min. The oxygen decrease in the seawater was defined as the rate of respiration after dark acclimation for 2 min, as described for the measurement of photosynthesis rates (Xu and Gao, 2012). The oxygen increase in the seawater was defined as the net photosynthetic rate after an increase in light density. Light density was described as μmol photons m^{-2} s^{-1} and adjusted by a double-ended halogen lamp (500 w, 230 v, PHILIPS, Jiangsu, China).

A photosynthesis-irradiation curve (P-E curve) was also obtained during 30 min under different irradiances (100, 200, 300, 400, 500, and 600 μmol photons m^{-2} s^{-1}) and durations of light irradiation.

The maximum net photosynthetic rate (P_{max}) and the photosynthetic efficiency (α) were calculated using the following equation:

$$P = P_{max} \times \tanh(\alpha \times E / P_{max}) + R_d, \quad (2)$$

where P represents the photosynthetic rate and R_d represents the

respiration rate.

2.4. Chlorophyll fluorescence measurement

Chlorophyll fluorescence was measured by a pulse modulation fluorometer (Water-PAM, Walz, Germany) as described in Enríquez and Borowitzka (2011). After dark acclimation for 15 min at the culture temperature, the relative electron transfer rate (rETR) and non-photochemical quenching (NPQ) were measured under culture light intensity (150 μmol photons m^{-2} s^{-1}) for 60 and 148 s. The fitting formula was used according to Genty et al. (1989):

$$rETR = yield \times 0.5 \times PAR, \quad (3)$$

where yield represents the effective photosynthetic quantum yield of PSII in response to light irradiation, 0.5 is the proportion of absorbed light to the total incident light, and PAR represents actinic light intensity.

The NPQ was calculated as follows:

$$NPQ = (Fm - Fm') / Fm', \quad (4)$$

where Fm represents the maximum chlorophyll fluorescence after dark acclimation, and Fm' represents the maximum fluorescence yield in light.

The rapid light curves were measured under nine different photosynthetically active radiation levels (PAR: 25, 81, 120, 184, 272, 415, 619, 878, and 1,218 μmol photons m^{-2} s^{-1}) for rETR. Subsequently, the maximum rETR ($rETR_{max}$) and the light use efficiency (α) of algae were obtained by nonlinear fitting of the rapid light curves of rETR. The following fitting formula was used (Jassby and Platt, 1976; Eilers and Peeters 1988):

$$rETR = rETR_{max} \times \tanh(\alpha \times E / rETR_{max}), \quad (5)$$

where E represents the incident irradiance.

2.5. Pigment contents

We dissolved 0.02 g of thalli (fresh weight) in 5 mL of anhydrous methanol at 4 °C for 24 h in darkness to complete the extraction. The absorbance of the samples was measured at 750, 665, and 652 nm using a UV spectrophotometer. The contents of Chl *a* and chlorophyll *b* (Chl *b*) were calculated as described by Porra et al. (1989):

$$Chl\ a = 16.29 \times A665.2–8.54 \times A652.0 \quad (6)$$

$$Chl\ b = 30.66 \times A652.0–13.58 \times A665.2 \quad (7)$$

2.6. Data analysis

The results are expressed as mean values ± standard deviation. For each parameter under the same CO_2 concentration but at different Cu conditions, we used one-way ANOVA to determine the differences. The effects of oceanic acidification and Cu concentrations on RGR, NPQ, rETR, net photosynthetic rate, respiration rate, Chl *a*, Chl *b*, and Chl *a/b* were analyzed by two-way analysis of variance (ANOVA). Tukey's honestly significant difference (HSD) analysis was conducted for *post-hoc* investigation. For all analyses, we used the Origin 9.0 software with a 95% confidence interval.

3. Results

3.1. Length and RGR of juvenile and adult stages

With increasing Cu levels, the life cycle of thalli was prolonged, and at LCu and MCu, the algae began to die after 15 days; at HCu, the algae began to die after 17 days under high CO_2 levels (Fig. 1A). Two-way ANOVA showed that Cu and CO_2 had significant interactions; both Cu and CO_2 also exerted a main effect on the RGR of *U. linza* at the juvenile stage ($p < 0.001$) (Fig. 1B, Table 2). The RGR decreased with increasing Cu concentrations at all conditions under high CO_2 levels (Fig. 1B). However, at atmospheric CO_2 concentration, the RGR at the juvenile stage increased with increasing Cu concentrations (Fig. 1B). A similar trend was found for the adult stage. Two-way ANOVA showed that Cu and CO_2 had a significant interaction; both Cu and CO_2 also exerted main effects on the RGR of *U. linza* at the adult stage ($p < 0.001$) (Fig. 1C, Table 2). At high CO_2 levels, the RGR increased at MCu and then decreased at HCu compared with the control (LCu) (Fig. 1C). At atmospheric CO_2 concentration, the RGR was also increased at MCu and HCu compared with the control (LCu) (Fig. 1C). Both Cu and CO_2 had an interactive effect, and each of them exerted a main effect on RGR based on the mass (RGR_{mass}) of *U. linza* at the late adult stage as analyzed by two-way ANOVA ($p < 0.001$) (Fig. 1D, Table 2). The RGR_{mass} decreased at HCu compared with the control (LCu) under high CO_2 concentrations. A significant difference in RGR_{mass} was observed at HCu between atmospheric and high CO_2 concentrations. With increasing Cu concentrations, no significant difference was observed for RGR_{mass} at atmospheric CO_2 level (Fig. 1D).

3.2. Photosynthesis and respiration measurement

We observed no interactive effects of CO_2 and Cu ($p = 0.09$), and Cu exerted a main effect on the net photosynthetic rate of *U. linza* (Fig. 2A, Table 3). At the high CO_2 level, the net photosynthetic rate of *U. linza* decreased with increasing Cu concentrations. It decreased to 180.80 and 165.54 μM O_2 g^{-1} FW h^{-1} at high CO_2 concentrations at MCu and HCu, respectively. However, the net photosynthetic rate significantly decreased from 215.43 ± 19.96 μM O_2 g^{-1} FW h^{-1} (LCu) to 171.11 ± 20.48 μM O_2 g^{-1} FW h^{-1} (MCu) and then increased to 200.81 ± 8.47 μM O_2 g^{-1} FW h^{-1} (HCu). No significant difference was found between atmospheric and high CO_2 levels ($p > 0.05$).

We found no interactive effects of Cu and CO_2 ($p < 0.001$) on respiration rate, and both Cu and CO_2 had a main effect on the respiration rate of *U. linza* (Fig. 2B, Table 3). With increasing Cu concentrations, the respiration rate of *U. linza* increased under high CO_2 levels from 42.04 ± 5.15 μM O_2 g^{-1} FW h^{-1} (MCu) to 61.53 ± 4.37 μM O_2 g^{-1} FW h^{-1} (HCu) under atmospheric CO_2 levels. A significant difference was observed at HCu at atmospheric and high CO_2 levels.

3.3. Chlorophyll fluorescence parameters

We observed an interactive effect of Cu and CO_2 concentrations on NPQ ($p = 0.02$), and each factor also had a main effect (Fig. 3A, Table 3). Both MCu and HCu decreased NPQ to 0.31 ± 0.07 and 0.40 ± 0.05, respectively, compared with that at LCu under the high CO_2 concentration (Fig. 3A). At atmospheric CO_2, MCu increased NPQ compared with the control (LCu). A significant difference was observed at MCu between atmospheric and high CO_2 levels on NPQ. We found an interactive effect of CO_2 and Cu ($p < 0.001$), and both factors exerted a main effect on the rETR of *U. linza* (Fig. 3B, Table 3). At high CO_2 concentrations, with increasing Cu levels, rETR decreased from 44.75 ± 6.20 (MCu) to 53.87 ± 2.59 (HCu). However, at atmospheric CO_2 concentration, no significant difference was observed for rETR with increased Cu levels ($p > 0.05$).

There was an interactive effect of CO_2 and Cu ($p < 0.001$) on $rETR_{max}$ of *U. linza*, and each factor also had a main effect (Fig. 4, Tables 1 and 3). The $rETR_{max}$ significantly decreased with increasing Cu under high CO_2 levels compared with atmospheric CO_2 concentration from 255.32 ± 25.89 μmol e^{-1} m^{-2} s^{-1} (LCu) to 123.16 ± 30.77 μmol e^{-1} m^{-2} s^{-1} (MCu) and 158.13 ± 13.93 μmol e^{-1} m^{-2} s^{-1} (HCu) at high CO_2 levels. Regarding α of *U. linza*, CO_2 and Cu had no interactive effect ($p < 0.001$), and each factor exerted a main effect on α (Fig. 4, Tables 1 and 3). No

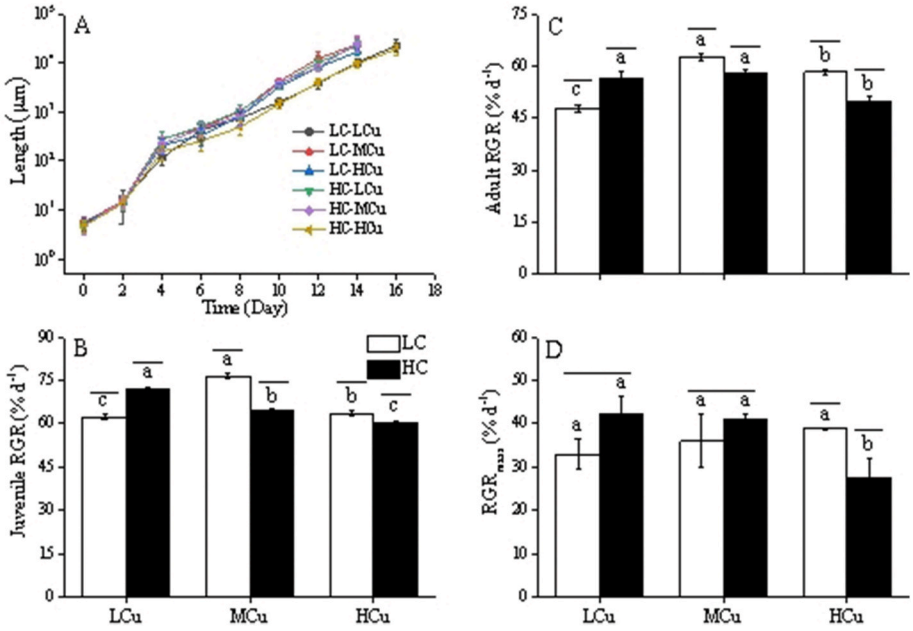

Fig. 1. Length (A), relative growth rate (RGR) at juvenile (B) and adult stages (C), and relative growth rate based on the mass (RGR_{mass}) at the late adult stage of *U. linza* grown at different Cu and CO_2 concentrations. LCu, Control; MCu, 0.125 μM; HCu, 0.25 μM. LC, 415 μatm CO_2; HC, 1,000 μatm CO_2. Values show mean ± SD. Different letters represent significant differences ($p < 0.05$) among the Cu concentrations at the same CO_2 concentration, and different symbols represent significant differences ($p < 0.05$) among the CO_2 concentrations at the same Cu concentration.

Table 1
Maximum relative electron transport rate ($rETR_{max}$) and electron transport efficiency (α) of *U. linza* at different Cu concentrations and CO_2 levels. LCu, Control; MCu, 0.125 μM; HCu, 0.25 μM. LC, 415 μatm CO_2; HC, 1,000 μatm CO_2. Different letters represent significant differences ($p < 0.05$) among Cu concentrations at the same CO_2 concentration. * indicates a significant difference ($p < 0.05$) between the CO_2 concentrations at the same Cu concentration.

	$rETR_{max}$ (μmol e^{-1} m^{-2} s^{-1})	α
LC-LCu	155.21 ± 36.68^{b*}	0.5 ± 0.07^{a*}
LC-MCu	224.35 ± 34.06^{a*}	0.49 ± 0.03a*
LC-HCu	222.63 ± 17.83^{a*}	0.51 ± 0.04^{a}
HC-LCu	255.32 ± 25.89^{a}	0.55 ± 0.04^{a}
HC-MCu	123.16 ± 30.77^{c}	0.41 ± 0.09^{c}
HC-HCu	158.13 ± 13.93^{b}	0.45 ± 0.02^{b}

significant difference was observed for α at atmospheric CO_2 level ($p > 0.05$), but it decreased significantly to 0.41 ± 0.09 and 0.45 ± 0.02, respectively, at MCu and HCu at high CO_2 concentrations (Table 1).

3.4. Pigment contents

We observed no interactive effect of CO_2 and Cu ($p = 0.42$) on Chl *a*, and neither of these factors exerted a main effect (Fig. 5A, Table 2). Under atmospheric CO_2, no significant difference was observed for the contents of Chl *an* at LCu and MCu. The Chl *a* content increased to 1.99 ± 0.10 mg g^{-1} (MCu) from 1.84 ± 0.13 mg g^{-1} (LCu). Under high CO_2 concentration,s with increasing Cu concentrations, the Chl *a* content increased from 1.17 ± 0.12 mg g^{-1} (LCu) to 1.78 ± 0.24 mg g^{-1} (HCu). A significant difference was observed at LCu and MCu between atmospheric and high CO_2 levels. There was no interactive effect of CO_2 and Cu on Chl *b* ($p = 0.21$), and neither factor exerted a main effect on Chl *b* (Fig. 5B, Table 2). No significant difference in the Chl *b* content was found for these Cu concentrations at atmospheric and high CO_2 concentrations. We found no interactive effect of CO_2 and Cu on the Chl *a*/*b* rate ($p = 0.11$), and only CO_2 exerted a main effect on this rate (Fig. 5C, Table 2). No significant difference in the Chl a/*b* rate was found for these Cu concentrations at atmospheric CO_2 and high CO_2 levels. The Chl a/*b* rate under high CO_2 levels was significantly lower than that under atmospheric CO_2.

4. Discussion

Based on our results, Cu and OA synergistically reduce the growth and photosynthetic performance of the green macroalga *Ulva linza*, prolonging its life cycle. These results might be due to the fact that Cu accelerates cell proliferation by inducing the conversion of the G0/G1 phase to the G2/M phase of the cell cycle, and the transcript levels of the cell division-related gene, *ftsHI*, was increased after exposure to 40 and 60 μM Cu, suggesting that the synthetic iron-sulfur clusters maintained an active cellular metabolism, allowing faster electron transfer processes and energy generation, but, most likely, facilitating cell damage (Wei et al., 2014). With increasing Cu concentrations, RGR_{length} decreased more than at LCu in both the juvenile and adult stages at high CO_2 levels. However, at the adult stage, no significant difference was observed between LCu and MCu under elevated CO_2 levels (Fig. 1B and C), suggesting that a higher tolerance to heavy metals at this stage. With increasing Cu concentrations, the life cycle of *U. linza* was prolonged, despite the slow growth of thalli at high CO_2 concentrations (Fig. 1A).

Table 2
Two-way analysis of variance for the effects of CO_2 and Cu on relative growth rate based on the length (RGR_{length}) at juvenile and adult stages and the relative growth rate based on the mass (RGR_{mass}) at the later adult stage, Chl *a*, Chl *b*, and Chl *a*/*b* of *U. linza* at different Cu and CO_2 concentrations. LCu, Control; MCu, 0.125 μM; HCu, 0.25 μM. LC, 415 μatm CO_2; HC, 1,000 μatm CO_2. df means degree of freedom, F means the value of F statistic, and Sig. means *p*-value.

Source	RGR_{length} at juvenile stage			RGR_{length} at adult stage			RGR_{mass} at later adult stage			Chl *a*			Chl *b*			Chl *a*/*b*		
	df	F	Sig.	df	F	Sig.	df	F	Sig.	df	F	Sig.	df	F	Sig.	df	F	Sig.
CO_2	1	6543.83	<0.001	1	1250.49	<0.001	1	219.27	<0.001	1	2.98	0.11	1	2.16	0.17	1	19.48	<0.001
Cu	2	9768.02	<0.001	2	1022.44	<0.001	2	105.40	<0.001	2	2.94	0.09	2	3.36	0.07	2	3.43	0.07
CO_2 × Cu	2	8066.40	<0.001	2	1004.58	<0.001	2	75.73	<0.001	2	0.94	0.42	2	1.79	0.21	2	2.64	0.11
Error	12			12			12			12			12			12		

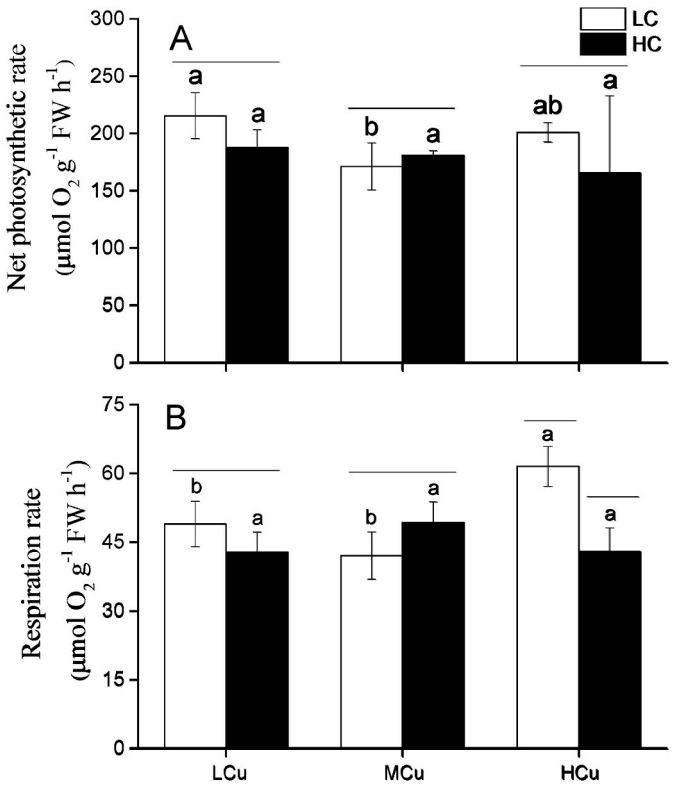

Fig. 2. Net photosynthetic and respiration rates of *U. linza* at different Cu and CO_2 concentrations. LCu, Control; MCu, 0.125 μM; HCu, 0.25 μM. LC, 415 μatm CO_2; HC, 1,000 μatm CO_2. Values show mean ± SD. Different letters represent significant differences ($p < 0.05$) among the Cu concentrations at the same CO_2 concentration, and different symbols represent significant differences ($p < 0.05$) among the CO_2 concentrations at the same Cu concentration.

Xu and Gao (2012) and Olischläger and Wiencke (2013) state that elevated CO_2 levels could promote the growth of *U. linza* and *Neosiphonia harveyi*. At HCu, the RGR of thalli clearly decreased at OA (Fig. 1B, C, D), especially at HCu during the adult stage (Fig. 1D). The heavy metal Cu mainly exists in the form of free ions in seawater, and its dominant complexes are CO_3^{2-} and OH^-. Elevating the CO_2 level will decrease the pH and lead to a decrease in CO_3^{2-} and OH^- levels in the seawater (MillerO et al., 2009). Increasing the Cu concentration would increase the number of free ions, resulting in an increasing toxicity of Cu for thalli (Gao et al., 2017).

Adenylate and pyridine nucleotides are key components of photosynthesis and respiration mechanisms; therefore, chloroplasts and mitochondria must be coordinated to optimize the energy metabolism (Dahal and Vanlerberghe, 2017). Once energy imbalances affect an organelle, the respective other factors will be offset by compensatory reactions (Dahal and Vanlerberghe, 2017). Mitochondrial respiration is an important physiological process for plants and required for most energy-dependent metabolic processes. It can dissipate excess energy in algae and alleviate the damage caused by Cu to algae (Dahal and Vanlerberghe, 2017). In our study, the respiration rate decreased more significantly at elevated CO_2 concentrations than at atmospheric CO_2 at HCu (Fig. 3B). However, no significant difference was observed both at MCu and HCu for respiration rate at high CO_2 concentrations, indicating that Cu toxicity is weakened by the effect of high CO_2 levels. No significant difference was observed for the net photosynthetic rate at MCu compared with that at LCu under high CO_2, most likely because of the alleviation of Cu toxicity effects under high CO_2 levels (Gao et al., 2017; Baumann et al., 2009). The content of Chl *a* was significantly increased at HCu compared with that at LCu and MCu under high CO_2 concentrations. These results suggested that Chl synthesis increases to alleviate the toxicity of Cu at increasing Cu levels, as reported elsewhere (Han et al., 2008). Chojnacka et al. (2005) suggest that the chlorophyll content increase is an adaptive strategy, where Mg^{2+} could exchange with intercellular Cu^{2+} to decrease the toxicity of Cu^{2+} in a blue-green alga (*Spirulina* sp.). In this context, the increase in chlorophyll content under higher Cu levels could as a way to replenish the chlorophyll pool affected by oxidative damage. Non-photochemical quenching was also increased at HCu, indicating that thalli dissipated excess light energy in the form of heat. Simultaneously, Chl *a*, as a light-capture pigment, was decreased to avoid overexcitation of the electron transport (Fig. 5A), as also described elsewhere (Xu and Gao, 2012). This was supported by the observed decrease in antenna size and the decrease in the Chl *a/b* ratio (Fig. 5C). However, the growth rate was significantly decreased under high CO_2 concentrations, although the Chl content, NPQ, and rETR were higher than at MCu, indicating that excess Cu damaged the protective mechanism. Although more energy was dissipated via heat, the high CO_2 levels destroyed the balance of acid-base at the cell surface, which exacerbated the toxicity of metal to cells (Gao et al., 2017). Copper is an essential trace element for both the growth and metabolism of algae and promotes the photosynthesis and growth of algae as an enzymatic cofactor. However, at high Cu levels, since most of the electron transfer carriers in the electron transport chain were iron-sulfur clusters, Cu was more significantly polarized than Fe and, therefore, more sulfhydryl-friendly than Fe; in this sense, Cu competitively combines with sulfur. Consequently, the carrier in the electron transport chain became a "Cu-sulfur cluster", causing poor electron transport and electron spillover and combining with oxygen to form reactive oxygen species through the Fenton reaction, thus, causing oxidative damage to algae cells and inhibiting the respiratory chain-related gene (*nad5*, *SDH2*, and *cox3*) and the photosynthetic chain related gene (*psbD*, *petD*, *psaB*, and *peF*) expression (Wei et al., 2014). In response, the protein structure was damaged and enzyme activity was decreased, which ultimately affected growth (Halliwell and Gutteridge, 2015). In addition, Cu also combined with the chloroplast membrane and other cellular proteins, which led to chloroplast protein degradation and, eventually, death (Halliwell and Gutteridge, 2015). These results are consistent with Roberts et al. (2013), who reported that at high CO_2 levels, the toxicity of heavy metals to DNA and protein was more significant in *Corophium volutator*. These mechanisms might have contributed to a H^+-mediated exacerbation of the Cu concentration in the seawater, thus enhancing the toxicity of Cu to thalli, which cannot be offset through the competition effect between H^+ and Cu (Roberts et al., 2013).

We investigated the effect of OA on the photosynthetic response of

Table 3
Two-way analysis of variance for the effects of CO_2 and Cu on net photosynthetic and respiration rates, NPQ, rETR, maximum rETR ($rETR_{max}$), and electron transport efficiency (α) of *U. linza* at different Cu and CO_2 concentrations. LCu, Control; MCu, 0.125 μM; HCu, 0.25 μM. LC, 415 μatm CO_2; HC, 1,000 μatm CO_2. df means degree of freedom, F means the value of F statistic, and Sig. means *p*-value.

Source	Net photosynthetic rate			Respiration rate			NPQ			rETR			$rETR_{max}$			α		
	df	F	Sig.	df	F	Sig.	df	F	Sig.	df	F	Sig.	df	F	Sig.	df	F	Sig.
CO_2	1	10.62	<0.001	1	172.04	<0.001	1	10.00	0.01	1	62.72	<0.001	1	15.91	<0.001	1	3.67	0.06
Cu	2	8.12	<0.001	2	170.95	<0.001	2	6.46	0.01	2	32.16	<0.001	2	11.32	<0.001	2	15.88	<0.001
CO_2 × Cu	2	2.58	0.09	2	232.16	<0.001	2	5.95	0.02	2	100.21	<0.001	2	119.59	<0.001	2	13.71	<0.001
Error	12			12			12			12			12			12		

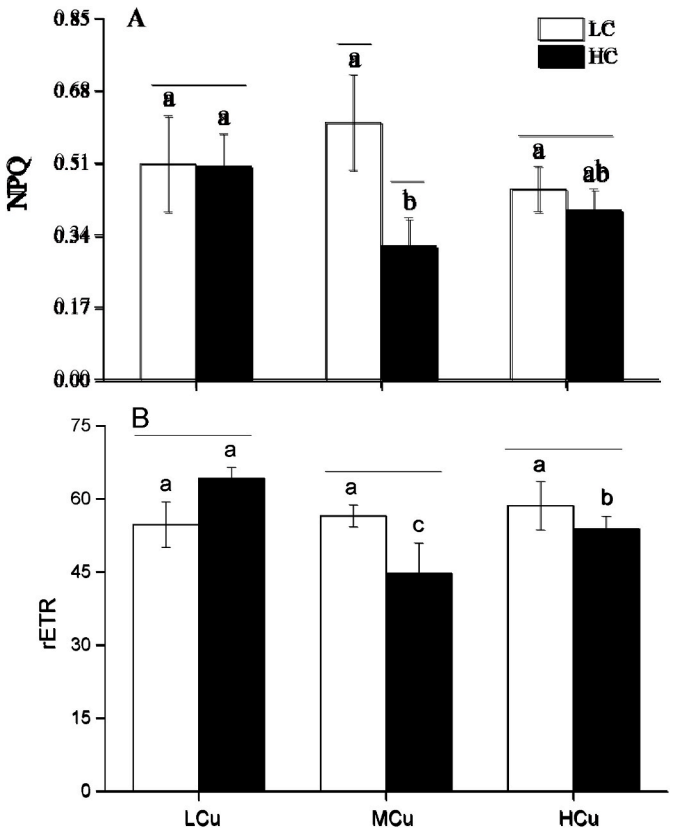

Fig. 3. Non-photochemical quenching (NPQ) and relative electron transfer rate (rETR) of *U. linza* at different Cu and CO_2 concentrations. LCu, Control; MCu, 0.125 μM; HCu, 0.25 μM. LC, 415 μatm CO_2; HC, 1,000 μatm CO_2. Values show mean ± SD. Different letters represent significant differences ($p < 0.05$) among the Cu concentrations at the same CO_2 concentration, and different symbols represent significant differences ($p < 0.05$) among the CO_2 concentrations at the same Cu concentration.

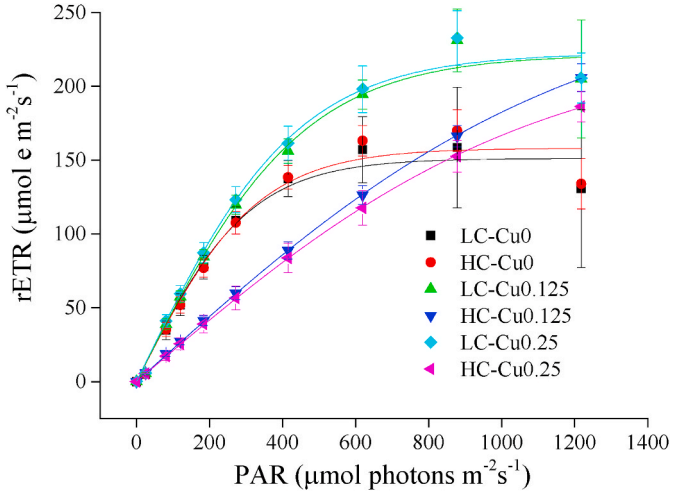

Fig. 4. Rapid light curve for *U. linza* for different Cu and CO_2 concentrations. LCu, Control; MCu, 0.125 μM; HCu, 0.25 μM. LC, 415 μatm CO_2; HC, 1,000 μatm CO_2. Error bars indicate SD (n = 3).

the green tide alga *U. linza* to Cu pollution. At a high Cu level, the damage caused by Cu to *U. linza* was enhanced in both juvenile and adult stages under high CO_2 concentrations compared with ambient CO_2. While the life cycle was prolonged at high Cu levels under high CO_2 concentrations, the growth of *U. linza* was inhibited, suggesting that the

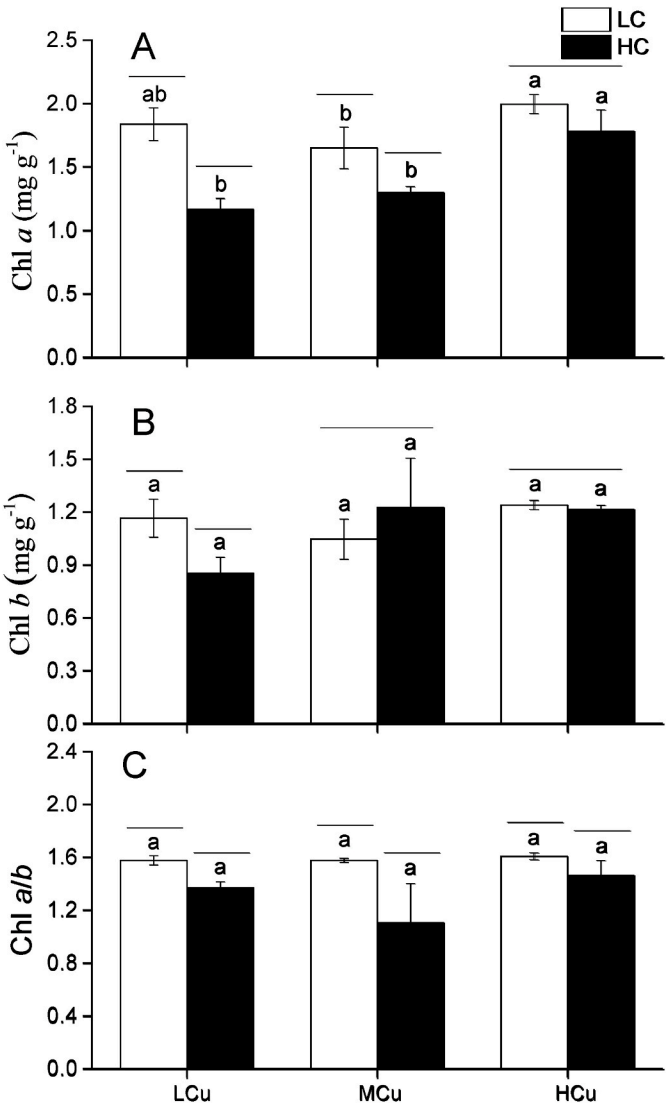

Fig. 5. Pigment contents of Chl *a* (A), Chl *b* (B), and Chl *a*/*b* rate (C) of *U. linza* at different Cu and CO_2 concentrations. LCu, Control; MCu, 0.125 μM; HCu, 0.25 μM LC, 415 μatm CO_2; HC, 1,000 μatm CO_2. Values show mean ± SD. Different letters represent significant differences ($p < 0.05$) among the Cu concentrations at the same CO_2 concentration, and different symbols represent significant differences ($p < 0.05$) among the CO_2 concentrations at the same Cu concentration.

alga can largely adapt to environmental changes. Against the background of a changing climate, the oceans will absorb significantly higher levels of CO_2 from the atmosphere, resulting in decreased pH values. This will exacerbate the damage Cu imposes on *U. linza* and further inhibit its growth, thus ultimately affecting the occurrence of green tide blooms.

CRediT authorship contribution statement

Tianpeng Xu: contributed to carrying out the experiments. **Junyang Cao:** contributed to carrying out the experiments. **Rui Qian:** contributed to carrying out the experiments. **Yujing Song:** contributed to carrying out the experiments. **Wen Wang:** contributed to carrying out the experiments. **Jing Ma:** Data curation, Writing – original draft, Writing – review & editing, contributed to carrying out the experiments, contributed to data analysis and paper writing. **Kunshan Gao:** Data curation, Writing – original draft, Writing – review & editing, contributed to experimental designs, contributed to data analysis and paper

writing. **Juntian Xu:** Data curation, Writing – original draft, Writing – review & editing, contributed to experimental designs, contributed to data analysis and paper writing.

Declaration of competing interest

The authors declare that they have no known competing financial interests or personal relationships that could have appeared to influence the work reported in this paper.

Acknowledgements

This study was supported by the special fund for Natural Resources Development (Innovation Project of Marine Science and Technology) of Jiangsu Province (JSZRHYKJ202001), the China Agriculture Research System (CARS50), the Modern Fisheries Industrial Research System of Jiangsu Province (JFRS-04), the China Postdoctoral Science Foundation (No. 2019M651431), Industry University Research Cooperation Project of Jiangsu Province (BY2020575), the Postdoctoral Science Foundation of Jiangsu Province (2018K150C), the Postdoctoral Science Foundation of Lianyungang, and the Priority Academic Program Development of Jiangsu Higher Education Institutions and Postgraduate research & Practice Innovation Program of Jiangsu Province (KYCX20_2889).

Appendix A. Supplementary data

Supplementary data to this article can be found online at https://doi.org/10.1016/j.marenvres.2021.105447.

References

Andrade, L.R., Farina, M., Filho, G.M.A., 2004. Effects of copper on *Enteromorpha flexuosa* (Chlorophyta) in vitro. Ecotoxicol. Environ. Saf. 58 (1), 117–125.

Bao, M.L., Wang, J.H., Xu, T.P., Wu, H.L., Li, X.S., Xu, J.T., 2019. Rising CO_2 levels alter the responses of the red macroalga *Pyropia yezoensis* under light stress. Aquaculture 501, 325–330.

Baumann, H.A., Morrison, L., Stengel, D.B., 2009. Metal accumulation and toxicity measured by PAM-chlorophyll fluorescence in seven species of marine macroalgae. Ecotoxicol. Environ. Saf. 72 (4), 1063–1075.

Boyer, G.L., Brand, L.E., 1998. Trace elements and harmful algal blooms. Nato Asi Series G: Ecol. Sci. 41 (1), 489–508.

Chojnacka, K., Chojnacki, A., Gorecka, H., 2005. Biosorption of Cr^{3+}, Cd^{2+} and Cu^{2+} ions by blue-green algae *Spirulina* sp.: kinetics, equilibrium and the mechanism of the process. Chemosphere 59 (1), 75–84.

Dahal, K., Vanlerberghe, G.C., 2017. Alternative oxidase respiration maintains both mitochondrial and chloroplast function during drought. New Phytol. 213 (2), 560–571.

Doney, S.C., Fabry, V.J., Feely, R.A., Kleypas, J.A., 2009. Ocean acidification: the other CO_2 problem. Ann. Rev. Mar. Sci. 1, 169–192.

Eilers, P.H.C., Peeters, J.C.H., 1988. A model for the relationship between light intensity and the rate of photosynthesis in phytoplankton. Ecol. Model. 42, 199–215.

Enríquez, S., Borowitzka, M.A., 2011. The use of the fluorescence signal in studies of seagrasses and macroalgae. Chlorophyll a Fluoresc. Aquat. Sci. Methods Appl. 4, 187–208.

Figueira, P., Henriques, B., Teixeira, A., Lopes, C.B., Reis, A.T., Monteiro, R., Duarte, A. C., Pardal, M.A., Pereira, E., 2016. Comparative study on metal biosorption by two macroalgae in saline waters: single and ternary systems. Environ. Sci. Pollut. Res. Int. 23 (12), 11985–11997.

Gaitán-Espitia, J.D., Hancock, J.R., Padilla-Gamiño, J.L., Rivest, E.B., Blanchette, C.A., Reed, D.C., Hofmann, G.E., 2014. Interactive effects of elevated temperature and pco2 on early-life-history stages of the giant kelp *Macrocystis pyrifera*. J. Exp. Mar. Biol. Ecol. 457, 51–58.

Gao, K.S., Aruga, Y., Asada, K., Ishihara, T., Akano, T., Kiyohara, M., 1991. Enhanced growth of the red alga *Porphyra yezoensis* Ueda in high CO_2 concentrations. J. Appl. Phycol. 3, 355–362.

Gao, S., Chen, X.Y., Yi, Q.Q., Wang, G.C., Pan, G.H., Lin, A.P., Peng, G., 2010. A strategy for the proliferation of *Ulva prolifera*, main causative species of green yides, with formation of sporangia by fragmentation. PloS One 5 (1), e8571.

Gao, K.S., Xu, J.T., Gao, G., Li, Y.H., Hutchins, D.A., Huang, B.Q., Wang, L., Zheng, Y., Jin, P., Cai, X.N., Häder, D.P., Li, W., Xu, K., Liu, N.N., Riebesell, U., 2012. Rising CO_2 and increased light exposure synergistically reduce marine primary productivity. Nat. Clim. Change 2 (7), 519–523.

Gao, G., Liu, Y., Li, X.S., Feng, Z.H., Xu, J.T., 2016a. An ocean acidification acclimatised green tide alga is robust to changes of seawater carbon chemistry but vulnerable to light stress. PloS One 11 (12), e0169040.

Gao, G., Zhong, Z.H., Zhou, X.H., Xu, J.T., 2016b. Changes in morphological plasticity of *Ulva prolifera* under different environmental conditions: a laboratory experiment. Harmful Algae 59, 51–58.

Gao, G., Liu, Y.M., Li, X.S., Feng, Z.H., Xu, Z.G., Wu, H.Y., Xu, J.T., 2017. Expected CO_2-induced ocean acidification modulates copper toxicity in the green tide alga *Ulva prolifera*. Environ. Exp. Bot. 135, 63–72.

Gao, G., Beardall, J., Bao, M.L., Wang, C., Ren, W.W., Xu, J.T., 2018. Ocean acidification and nutrient limitation synergistically reduce growth and photosynthetic performances of a green tide alga *Ulva linza*. Biogeosciences 15 (11).

Gao, G., Qu, L.M., Xu, T.P., Burgess, J.G., Xu, J.T., 2019. Future CO_2-induced ocean acidification enhances resilience of a green tide alga to low-salinity stress. ICES (Int. Counc. Explor. Sea) J. Mar. Sci. https://doi.org/10.1093/icesjms/fsz135.

Genty, B., Briantais, J.M., Baker, N.R., 1989. The relationship between the quantum yield of photosynthetic electron transport and quenching of chlorophyll fluorescence. BBA-Gen Subjects 990, 87–92.

Golubkov, S.M., Berezina, N.A., Gubelit, Y.I., Demchuk, A.S., Golubkov, M.S., Tiunov, A. V., 2018. A relative contribution of carbon from green tide algae *Cladophora glomerata* and *Ulva intestinalis* in the coastal food webs in the Neva Estuary (Baltic Sea). Mar. Pollut. Bull. 126, 43–50.

Hall-Spencer, J.M., Harvey, B.P., 2019. Ocean acidification impacts on coastal ecosystem services due to habitat degradation. Emerg. Topics Life Sci. 3 (2), 197–206.

Hall-Spencer, J.M., Rodolfo-Metalpa, R., Martin, S., Ransome, E., Fine, M., Turner, S.M., Rowley, S.J., Tedesco, D., Buia, M.C., 2008. Volcanic carbon dioxide vents show ecosystem effects of ocean acidification. Nature 454, 96–99.

Halliwell, B., Gutteridge, J.M.C., 2015. Free Radicals in Biology and Medicine. Oxford University Press, USA.

Han, T., Kang, S.H., Park, J.S., Lee, H.K., Brown, M.T., 2008. Physiological responses of *Ulva pertusa* and *U. armoricana* to copper exposure. Aquat. Toxicol. 86 (2), 176–184.

Hoffmann, L.J., Breitbarth, E., Boyd, P.W., Hunter, K.A., 2012. Influence of ocean warming and acidification on trace metal biogeochemistry. Mar. Ecol. Prog. Ser. 470, 191–205.

Iheanacho, E.U., Ndulaka, J.C., Onuh, C.F., 2017. Environmental pollution and heavy metals. Euro. J. Biotechnol. Biosci. 5, 73–78.

Isari, S., Zervoudaki, S., Peters, J., Papantoniou, G., Pelejero, C., Saiz, E., 2015. Lack of evidence for elevated CO_2-induced bottom-up effects on marine copepods: a dinoflagellate-calanoid prey-predator pair. ICES (Int. Counc. Explor. Sea) J. Mar. Sci. 73, 650–658.

Ismail, G.A., Ismail, M.M., 2017. Variation in oxidative stress indices of two green seaweeds growing under different heavy metal stresses. Environ. Monit. Assess. 189 (2), 68–80.

Jassby, A.D., Platt, T., 1976. Mathematical formulation of the relationship between photosynthesis and light for phytoplankton. Limnol. Oceanogr. 21 (4), 540–547.

Ji, Y., Gao, K.S., 2020. Effects of climate change factors on marine macroalgae: a review-sciencedirect. Adv. Mar. Biol. 88, 91–136.

Kang, E.J., Han, A.R., Kim, J.H., Kim, I.N., Kim, C., 2021. Evaluating bloom potential of the green-tide forming alga *Ulva ohnoi* under ocean acidification and warming. Sci. Total Environ. https://doi.org/10.1016/j.scitotenv.

Koch, M., Bowes, G., Ross, C., Zhang, X.H., 2013. Climate change and ocean acidification effects on seagrasses and marine macroalgae. Global Change Biol. 19 (1), 103–132.

Leal, P.P., Hurd, C.L., Sander, S.G., Armstrong, E., Roleda, M.Y., 2016. Copper ecotoxicology of marine algae: a methodological appraisal. Chem. Ecol. 32, 786–800.

Leusch, A., Holan, Z.R., Volesky, B., 1995. Biosorption of heavy metals (Cd, Cu, Ni, Pb, Zn) by chemically-reinforced biomass of marine algae. J. Chem. Technol. Technol. Biotechnol. 62 (3), 279–288.

MillerO, F.J., Woosley, R., DiTrolio, B., Waters, J., 2009. Effect of ocean acidification on the speciation of metals in seawater. Oceanography 22 (4), 72–85.

Mirzaei, M.R., Azini, M.R., Rad, T.A., 2016. Seasonal variation of heavy metal in seawater, sediment and hooded oyster, Saccostrea cucullata. In: Iranian Southern Waters (Chabahar Coast).

Naser, H.A., 2013. Assessment and management of heavy metal pollution in the marine environment of the Arabian Gulf: a review. Mar. Pollut. Bull. 72 (1), 6–13.

Ndu, U., Barkay, T., Schartup, A.T., Mason, R.P., Reinfelder, J.R., 2016. The effect of aqueous speciation and cellular ligand binding on the biotransformation and bioavailability of methylmercury in mercury-resistant bacteria. Biodegradation 27 (1), 29–36.

Olischläger, M., Wiencke, C., 2013. Ocean acidification alleviates low-temperature effects on growth and photosynthesis of the red alga *Neosiphonia harveyi* (Rhodophyta). J. Exp. Bot. 64 (18), 5587–5597.

Porra, R.J., Thompson, W.A., Kriedemann, P.E., 1989. Determination of accurate extinction coefficients and simultaneous equations for assaying chlorophylls *a* and *b* extracted with four different solvents: verification of the concentration of chlorophyll standards by atomic absorption spectroscopy. Biochim. Biophys. Acta Bioenerg. 975 (3), 384–394.

Qu, L.M., Xu, J.T., Sun, J.Z., Li, X.S., Gao, K.S., 2017. Diurnal pH fluctuations of seawater influence the responses of an economic red macroalga *Gracilaria lemaneiformis* to future CO_2 -induced seawater acidification. Aquaculture 473, 383–388.

Richards, R., Chaloupka, M., Sanò, M., Tomlinson, R., 2011. Modelling the effects of 'coastal'acidification on copper speciation. Ecol. Model. 222 (19), 3559–3567.

Roberts, D.A., Birchenough, S.N., Lewis, C., Sanders, M.B., Bolam, T., Sheahan, D., 2013. Ocean acidification increases the toxicity of contaminated sediments. Global Change Biol. 19 (2), 340–351.

Schlüter, L., Lohbeck, K.T., Gröger, J.P., Riebesell, U., Reusch, T.B.H., 2016. Long-term dynamics of adaptive evolution in a globally important phytoplankton species to ocean acidification. Sci. Adv. 2 (7), 1501660–e1501668.

Shi, M.J., Wei, X.Y., Xu, J., Chen, B.J., Zhao, D.Y., Cui, S., Zhou, T., 2017. Carboxymethylated degraded polysaccharides from *Enteromorpha prolifera*: preparation and *in vitro* antioxidant activity. Food Chem. 215, 76–83.

Stocker, T.F., Qin, D., Plattner, G.K., Tignor, M.M.B., Allen, S.K., Boschung, J., A Nauels, A., Xia, Y., Bex, V., Midgley, P.M., 2014. Climate Change 2013: the Physical Science Basis. Contribution of Working Group I to the Fifth Assessment Report of the Intergovernmental Panel on Climate Change.

Wang, H., Wang, G.C., Gu, W.H., 2020. Macroalgal blooms caused by marine nutrient changes resulting from human activities. J. Appl. Ecol. 57 (4), 766–776.

Wei, Y., Zhu, N., Lavoie, M., Wang, J.Y., Qian, H.F., Fu, Z.W., 2014. Copper toxicity to phaeodactylum tricornutum: a survey of the sensitivity of various toxicity endpoints at the physiological, biochemical, molecular and structural levels. Biometals 27 (3), 527–537.

Xu, J.T., Gao, K.S., 2012. Future CO_2-induced ocean acidification mediates the physiological performance of a green tide alga. Plant Physiol. 160 (4), 1762–1769.

Yue, F., Gao, G., Ma, J., Wu, H.L., Li, X.S., Xu, J.T., 2019. Future CO_2-induced seawater acidification mediates the physiological performance of a green alga *Ulva linza* in different photoperiods. PeerJ 7, e7048.

Zeng, X.F., Chen, X.J., Zhuang, J., 2015. The positive relationship between ocean acidification and pollution. Mar. Pollut. Bull. 91 (1), 14–21.